International Journal of Control
Vol. 00, No. 00, DD Month 200x, 1–13

Hybrid Model Predictive Control Application Towards Optimal Semi-Active Suspension

N. Giorgetti†, A. Bemporad†, E. Tseng‡, D. Hrovat‡

†Dept. Information Engineering, University of Siena, Italy, {giorgetti,bemporad}@dii.unisi.it
‡Ford Research Laboratories, Dearborn (MI), USA, {htseng,dhrovat}@ford.com

(*Received 00 Month 200x; In final form 00 Month 200x*)

The optimal control problem of a quarter-car semi-active suspension has been studied in the past. Considering that a quarter-car semi-active suspension can either be modeled as a linear system with state dependent constraint on control (of actuator force) input, or a bi-linear system with a control (of variable damping coefficient) saturation, the seemingly simple problem poses several interesting questions and challenges. Does the saturated version of the optimal control law derived from the corresponding un-constrained system, i.e. "clipped-optimal", remain optimal for the constrained case as suggested in some previous publications? Or should the optimal deviate from the "clipped-optimal" as suggested in other publications? If the optimal control law of the constrained system does deviate from its un-constrained counter-part, how different are they? What is the structure of the optimal control law? Does it retain the linear state feedback form (as the unconstrained case)? In this paper, we attempt to answer some of the above questions by utilizing the recent development in model predictive control (MPC) of hybrid dynamical systems.

The constrained quarter-car semi-active suspension is modeled as a switching affine system, where the switching is determined by the activation of passivity constraints, force saturation, and maximum power dissipation limits. Theoretically, over an infinite prediction horizon the MPC controller corresponds to the exact optimal controller. The performance of different finite-horizon hybrid MPC controllers is tested in simulation using mixed-integer quadratic programming. Then, for short-horizon MPC controllers, we derive the explicit optimal control law and show that the optimal control is piecewise affine in state. In the process, we show that for horizon equal to one the explicit MPC control law corresponds to clipped LQR as expected. We also compare the derived optimal control law to various semi-active control laws in the literature including the well-known "clipped-optimal". We evaluate their corresponding performances for both a deterministic shock input case and a stochastic random disturbances case through simulations.

1 Introduction

For a quarter-car suspension problem, its ride and handling performance can be quantified based on the ℓ_2 norm of its states and output [1]. Therefore, linear optimal control theory such as LQ control can be applied to an (un-constrained) active suspension problem. [2–4] suggested a semi-active controller by passing the optimal active force through a limiter. This control law is known as the "clipped optimal" law. The question arises if the "clipped-optimal" is still optimal for the constrained case as suggested in some previous publications (described in [1]). Or should the optimal deviate from the "clipped-optimal" as suggested in other publications [5, 6]? If the optimal control law of the constrained system does deviate from its un-constrained counter-part, how different are they? And what would be the structure of the optimal control law?

Different attempts have been made over the years to answer the questions arisen above. For a deterministic road disturbance case, the existence of the optimal semi-active control based on two point boundary problem has been shown in [5]. [6] showed that the clipped optimal law cannot be optimal and postulated that the constrained optimal control maintains a linear feedback form. However, the solution of optimal control in [6] involves switching among three state dependent Riccati equations and must be done through off-line iterations. To date, to the author's knowledge, no explicit optimal control law for semi-active suspension has been shown.

In this paper, we address the above optimal semi-active suspension problem in the context of model predictive control (MPC) of hybrid systems. We derived explicit optimal control law for the deterministic case. Hybrid systems are characterized by the interaction between continuous states, whose dynamics

This work was supported by the HYCON Network of Excellence, contract number FP6-IST-511368.

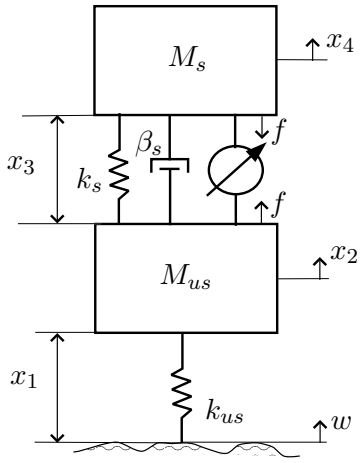

Figure 1. Two degree of freedom quarter car model

is governed by differential or difference equations, and discrete states, whose dynamics is described by finite state machines, logic rules, if-then-else conditions, etc. Typically, different continuous dynamics (or "modes") are associated with different discrete states and discrete inputs, and mode transitions (or "switches") are triggered by variables crossing specific thresholds (state events), by the elapse of certain time periods (time events), or by external decisions (input events) [7]. The MPC control strategy consists of solving at each sampling time, starting at the current state, an open-loop optimal control problem over a finite horizon. At the next time step the optimal control problem is solved starting from the new state and over a shifted horizon, leading to a moving horizon policy.

Recently, in [8–10] optimal control problems for discrete-time hybrid systems were solved by modeling the hybrid system as a mixed logical dynamical (MLD) system. This consists of a set of linear equalities and inequalities involving both real and (0-1) variables, so that the MPC control problem can be solved by a mixed-integer programming (MIP) solver. Despite the fact that efficient MIP solvers exist, on-line implementation of hybrid MPC control may require a substantial computational effort. This is usually acceptable in simulation while tuning the controller, but inadequate in fast-sampling automotive applications. In [10] and [11], it was shown that the MPC control law can be expressed explicitly as a collection of affine state feedback control gains and of corresponding polyhedral cells in the state-space: the cell the current state belongs to determines the corresponding gain to be applied. In this way, the computational burden associated with the hybrid-MPC controller becomes that of a lookup-table of linear gains.

The results of this paper appeared in preliminary form in the conference paper [12].

An optimal semi-active suspension problem is described in Section 2 where the performance index and constraints are defined. Section 3 reviews two constant (i.e. non-time varying nor state dependent) feedback gain control laws discussed in previous literature and illustrated how the "clipped optimal" solution is not the optimal one. In Section 4, the constrained quarter-car semi-active suspension was modeled as a switching affine system, where the switching is determined by the activation of passivity constraints, force saturation, and maximum dissipation limits. Section 5 discusses the explicit control law by solving the switching affine system through model predictive/hybrid control and shows the MPC results compared to the well-known "clipped optimal" control law.

2 Semi-Active Suspension Model and Constrained Optimization Problem

2.1 *Quarter Car Model*

A two degree of freedom quarter car model equipped with an adjustable force element is considered here, see Figure 1. With the assumptions that the springs and damping are linear and the tire damping is negligible and with the help of bond graph analysis, the active suspension system can be represented

mathematically as

$$\dot{x} = Ax + B\bar{f} + B_w w \tag{1}$$

where $x = [x_1,\ x_2,\ x_3,\ x_4]' \in \mathbb{R}^4$, x_1 [m] is the tire deflection from equilibrium, x_2 [m/s] is the unsprung mass velocity, x_3 [m] is the suspension deflection from equilibrium, x_4 [m/s] is the sprung mass velocity, $\bar{f}$ [N/Kg] is the normalized adjustable force, w [m/s] is the road velocity disturbance,

$$A = \begin{bmatrix} 0 & 1 & 0 & 0 \\ -\omega_{us}^2 & -2\rho\zeta\omega_s & \rho\omega_s^2 & 2\rho\zeta\omega_s \\ 0 & -1 & 0 & 1 \\ 0 & 2\zeta\omega_s & -\omega_s^2 & -2\zeta\omega_s \end{bmatrix}, \tag{2}$$

$$B = \begin{bmatrix} 0 \\ \rho \\ 0 \\ -1 \end{bmatrix}, \quad B_w = \begin{bmatrix} -1 \\ 0 \\ 0 \\ 0 \end{bmatrix}, \tag{3}$$

with

$$\rho = \frac{M_s}{M_{us}}, \qquad \omega_{us} = \sqrt{\frac{k_{us}}{M_{us}}}, \tag{4}$$

$$\omega_s = \sqrt{\frac{k_s}{M_s}}, \qquad \zeta = \frac{\beta_s}{2\sqrt{M_s k_s}}, \tag{5}$$

$$\bar{f} = \frac{f}{M_s}, \tag{6}$$

where M_{us} [kg] is the unsprung mass, M_s [kg] is the sprung mass, k_s [kg/s^2] is the suspension spring constant, k_{us} [kg/s^2] is the unsprung mass constant, and β_s [kg/s] is the suspension damping coefficient.

2.2 *Constrained Optimization Problem*

If we consider only adjustable force elements that is constrained by passivity, we have to impose on the model (1) the passivity constraint

$$\bar{f}(x_4 - x_2) \geq 0. \tag{7}$$

To illustrate the deviation of the constrained optimal from clipped optimal, we further restrict the maximum magnitude that can be generated by the adjustable semi-active force elements, that is, we consider the saturation constraint

$$|\bar{f}| \leq \sigma, \tag{8}$$

where σ is a constant indicating the maximum force capacity.

Maximum dissipating power constraint is also considered:

$$0 \leq \bar{f}(x_4 - x_2) \leq (2 \cdot \zeta_{max} \cdot \omega_s)(x_4 - x_2)^2, \tag{9}$$

where $\zeta_{max} = 25.5$ is the maximum damping ratio.

The objective of our problem is to control the constrained adjustable force element to minimize the suspension performance defined as [1]

$$\begin{aligned} J &= \int (q_1 x_1^2 + q_3 x_3^2 + \dot{x}_4^2) dt \\ &= \int (x^T Q x + \dot{x}_4^2) dt, \end{aligned} \tag{10}$$

where

$$Q = \begin{bmatrix} q_1 & 0 & 0 & 0 \\ 0 & 0 & 0 & 0 \\ 0 & 0 & q_3 & 0 \\ 0 & 0 & 0 & 0 \end{bmatrix}. \tag{11}$$

Performance index (11) is a combination of the RMS value of tire deflections, suspension displacements, and sprung mass accelerations that indicates road holding, packaging, and comfort respectively. We see that our semi-active suspension optimization problem can be viewed as the optimal control problem of a linear system under linear (8) and nonlinear (7), (9) constraints.

3 Linear Constant Feedback Gain Control for Sub-Optimal Semi-Active Suspensions

3.1 *Clipped-Optimal (Clipped-LQR)*

A way to look at the constrained optimization problem is noting the relation between the performance of the optimal active suspension and that of any semi-active suspension [6]:

$$J_{\text{semi}} = J_{\text{active,LQR}} + \int_0^\infty (\bar{f}_a - \bar{f})^2 dt, \tag{12}$$

where

$$J_{\text{active,LQR}} = x_0^T P_a x_0, \tag{13}$$

$$\bar{f}_a = (B^T P_a + S_0) x, \tag{14}$$

$$S_0 = B_4 A_{(4,:)}, \tag{15}$$

(where B_4 is the 4th element of vector B and $A_{(i,:)}$ is the i-th row of A), $x_0 \in \mathbb{R}^4$ is the initial condition, P_a is the solution of the Riccati equation

$$P_a(A - BS_0) + (A - BS_0)^T P_a = Q - (S_0^T S_0) + P_a B B^T P_a. \tag{16}$$

If one tries to minimize the integrand of the performance differences at every instant but not the whole integral, the control would attempt to follow the active force whenever it can. As a result, the corresponding desired semi-active force f is clipped whenever it exceeds its constraints due to either passivity or actuator limitations and can be expressed as

$$\begin{aligned} \bar{f}_{clipped-LQR} &= sat[\bar{f}_a] \\ &= sat[(B^T P_a + S_0)x] \\ &= sat[K_{LQ} x], \end{aligned} \tag{17}$$

where $sat[\cdot]$ operates on the commanded linear feedback term and saturated whenever it exceeds the constraints (8) and (9). Note that $B^T P_a x$ is the desirable total suspension force and $\bar{f}_p = -S_0 x$ is the passive suspension force from the passive spring and damper.

3.2 *Steepest Gradient Method*

Another way to look at the constrained optimization problem is noting the relation between the performance of a passive suspension and that of any semi-active suspension [6]:

$$\begin{aligned} J_{\text{semi}} &= J_{\text{passive}} + \int_0^\infty (-2\bar{f}(B^T P_L x + S_0 x) + \bar{f}^2)dt \\ &= J_{\text{passive}} + \int_0^\infty (-2\bar{f}(B^T P_L x - \bar{f}_p) + \bar{f}^2)dt \end{aligned} \tag{18}$$

Similarly, one can relate any semi-active suspension with the optimal passive suspension as

$$\begin{aligned} J_{\text{semi}} = J_{\text{passive,opt}} + \\ \int_0^\infty (-2\bar{f}(B^T P_{L,opt} x - \bar{f}_{p,opt}) + \bar{f}^2)dt, \end{aligned} \tag{19}$$

where

$$J_{\text{passive}} = x_0^T P_L x_0, \tag{20}$$

$$J_{\text{passive,opt}} = x_0^T P_{L,opt} x_0, \tag{21}$$

P_L is the solution of the Lyapunov equation,

$$A^T P_L + P_L^T A = Q + A_{(4,:)}^T A_{(4,:)}, \tag{22}$$

$P_{L,opt}$ is the solution of the Lyapunov equation,

$$A_{opt}^T P_L + P_L^T A_{opt} = Q + A_{opt,(4,:)}^T A_{opt,(4,:)}, \tag{23}$$

and A_{opt} is the A matrix with optimal damping, i.e., $\beta_s = \beta_{s,opt}$.

Since (19) relates the performance of the optimal passive suspension and that of a semi-active suspension, one can improve upon the optimal (damping) passive suspension by minimizing the second term in (19). If one minimizes the integrand of the performance differences at every instant (to be negative) but not necessarily the whole integral (due to state dependent constraint) in (19), the semi-active force which improves upon the optimal passive suspension can be expressed as

$$\begin{aligned} \bar{f}_{\text{SGM}} &= sat[B^T P_{L,opt} x - \bar{f}_{p,opt}] \\ &= sat[(B^T P_{L,opt} + S_{0,opt})x] \\ &= sat[K_{\text{SGM}} x] \end{aligned} \tag{24}$$

where $S_{0,opt} = B_4 A_{opt(4,:)}$ and $sat[\cdot]$ operates on the commanded adjustable force and saturates whenever it exceeds the constraints (8) and (9).

Table 1. Parameter values used in simulation

Parameter	Value	Description
T_s	10 ms	Sampling time
ω_s	1.5 Hz	Sprung mass natural frequency
ω_{us}	10 Hz	Wheel-hop natural frequency
ρ	10	Sprung-to-unsprung mass ratio
ζ	0	Damping ratio
σ	1	Maximum force capacity
q_1	1100	Weight on tire deflection
q_3	100	Weight on suspension deflection

3.3 *Simulation of Sub-Optimal Semi-Active Suspensions*

In this section, through two "shock tests" of different initial conditions, we illustrate that the "clipped optimal" solution is not the optimal one. To study the optimal semi-active suspension with on-line control implementations, discrete time simulations of sampling time T_s were considered and the weighting factors of design point "A" described in [1] were used (see Table 1). The semi-active suspension parameters studied are listed in Table 1 and the control feedback gains (described in Sections 3.1 and 3.2) for the discrete-time equivalent $(e^{T_s A}, \int_0^{T_s} e^{tA} B dt)$ of the semi-active system described by the matrices A and B defined in (2)–(3).

With the discrete-time implementation, for the "clipped optimal" control, we have,

$$K_{\mathrm{LQ}} = [-10.4748\ 0.2446\ 79.1519\ -3.9295]. \tag{25}$$

For the "steepest gradient" method, we have

$$K_{\mathrm{SGM}} = [1.5325\ 6.6053\ 43.8503\ -10.0321]. \tag{26}$$

Figure 2 shows a shock test with initial suspension deflection or a step change in suspension deflection defined by the initial condition $x_0 = [0,\ 0,\ 0.1,\ 0]'$. In Figure 2, we see that the "steepest gradient" method is 17% better (in terms of performance index) than the "clipped optimal" solution in this case. It should be pointed out that the amount of improvement is highly dependent on the initial condition and constraints. While the "clipped optimal" method is superior (in terms of the performance index) to the "steepest gradient" method in other simulation conditions, Figure 2 offers an important counter example that "clipped optimal" is at least 17% away from the true optimal in some cases.

Figure 3 shows a shock test with initial tire deflection or a step change in tire deflection defined by the initial condition $x_0 = [0.09\ 0\ 0\ 0]'$. In Figure 3 we see similarly that the "steepest gradient" method, being used as a counter example, illustrates that the "clipped optimal" solution is at least 16% away from the true optimal in this particular case.

It should be pointed out that the amount of performance differences is highly dependent on the initial condition and constraints. For example, Figure 4 shows "clipped optimal" out-performs the "steepest gradient" method in a different initial condition.

4 Hybrid Dynamical Model and Model Predictive Control

4.1 *Hybrid Dynamical Model*

The interest in hybrid systems is mainly motivated by the large variety of practical situations where physical processes interact with digital controllers, as for instance in embedded systems. Several modeling formalisms have been developed to describe hybrid systems [13,14], among them the class of Mixed Logical Dynamical (MLD) systems [8]. Examples of real-world applications that can be naturally modeled within the MLD framework are reported in [8, 15, 16]. The language HYSDEL (HYbrid Systems DEscription Language) was developed in [9] to obtain MLD models from of a high level textual description of the hybrid dynamics. HYSDEL models are used in the Hybrid Toolbox for Matlab$^{\mathrm{TM}}$ [10] for modeling, simulating,

and verifying the safety properties of hybrid systems, for designing MPC controllers for linear systems with constraints and hybrid systems, and for determining equivalent piecewise affine control functions that can be immediately prototyped on hardware.

In this section we explain how model (1) with constraints (7), (8) can be described as a hybrid dynamical system, and later we will show how the derived model can be used to define an optimal control policy which satisfies the passivity condition and a maximum dissipative constraint.

The nonlinear constraint (7) can be translated into a set of thresholds and logic conditions by introducing two binary variables δ_v, $\delta_{\bar{f}}$ such that

$$[\delta_v = 1] \leftrightarrow [x_4 - x_2 \geq 0], \tag{27a}$$

$$[\delta_{\bar{f}} = 1] \leftrightarrow [\bar{f} \geq 0], \tag{27b}$$

$$[\delta_v = 1] \rightarrow [\delta_{\bar{f}} = 1], \tag{27c}$$

$$[\delta_v = 0] \rightarrow [\delta_{\bar{f}} = 0]. \tag{27d}$$

The maximum dissipating power constraint (9) can be rewritten as

$$F = \begin{cases} \bar{f} - (2 \cdot 25.5 \cdot \omega_s)(x_4 - x_2) & \text{if } (x_4 - x_2) \leq 0 \\ -\bar{f} + (2 \cdot 25.5 \cdot \omega_s)(x_4 - x_2) & \text{otherwise} \end{cases} \tag{28a}$$

where $F \in \mathbb{R}$ is an auxiliary continuous variable on which is imposed the constraint

$$F \geq 0. \tag{28b}$$

By assigning

$$y = \frac{dx_4}{dt} = \begin{bmatrix} 0 & 2\zeta\omega_s & -\omega_s^2 & -2\zeta\omega_s \end{bmatrix} x - \bar{f} \tag{29}$$

as the output of the system, the discrete-time version of (1), obtained by sampling (1) with the sampling time T_s (see Table 1), constraints (27) and (28) are modeled as a hybrid system in HYSDEL [9]. Constraint (8) is included in the optimal control setup. The corresponding list is reported in the appendix. The HYSDEL compiler translates differences equations and constraints into the MLD system

$$x(t+1) = Ax(t) + B_1 u(t) + B_2 \delta(t) + B_3 z(t), \tag{30a}$$

$$y(t) = Cx(t) + D_1 u(t) + D_2 \delta(t) + D_3 z(t), \tag{30b}$$

$$E_2 \delta(t) + E_3 z(t) \leq E_1 u(t) + E_4 x(t) + E_5. \tag{30c}$$

In our case, $x = [x_1 \ x_2 \ x_3 \ x_4]' \in \mathbb{R}^4$, $y \in \mathbb{R}$, $u = [\bar{f}] \in \mathbb{R}$. The values of vectors $\delta(t)$ and $z(t)$ are, respectively, binary and real, and are determined uniquely by inequalities (30c) once $x(t)$ and $u(t)$ are fixed [8]. In our case the binary vector is $\delta = [\delta_v \ \delta_{\bar{f}}]' \in \{0,1\}^2$ and the continuous vector is $z = F \in \mathbb{R}$.

4.2 *Optimal Control Problem*

We describe how receding horizon optimal control for hybrid systems [8] can be usefully employed here to design a control law for the posed semiactive suspension control problem. The main idea is to setup a finite-horizon optimal regulation problem for the hybrid MLD system (30) by solving the following optimization

problem

$$\min_{\xi} J(\xi, x(t)) \triangleq x'_N Q_N x_N + \sum_{k=1}^{N-1} x'_k Q x_k + \sum_{k=0}^{N-1} y_k^2 \tag{31a}$$

$$\text{s. t. } \begin{cases} x_{k+1} = Ax_k + B_1 u_k + B_2 \delta_k + B_3 z_k \\ y_k = Cx_k + D_1 u_k + D_2 \delta_k + D_3 z_k \\ E_2 \delta_k + E_3 z_k \leq E_1 u_k + E_4 x_k + E_5 \\ x_0 = x(t) \end{cases} \tag{31b}$$

at each time step t, where $x(t)$ is the state of the MLD system at time t, $\xi \triangleq [u'_0, \ldots, u'_{N-1}, \delta'_0, \ldots, \delta'_{N-1}, z'_0, \ldots, z'_{N-1}]'$, and Q is defined as in (11). According to the so called "receding horizon" philosophy, the first move u_0^* of an optimizer ξ^* of (31) defines the current input:

$$u(t) = u_0^*. \tag{31c}$$

The terminal weight Q_N is defined as the Riccati matrix associated with the infinite horizon cost

$$\min \sum_{k=0}^{\infty} x'_k Q x_k + y_k^2 \tag{32}$$

where x_k, y_k are the states and output, respectively, of the discrete-time equivalent of the semiactive suspension system described by matrices A and B in (2)–(3). The corresponding LQR gain was reported in (25).

Using the Hybrid Toolbox [10], problem (31) is translated into a mixed integer quadratic program (MIQP), i.e., into the minimization of a quadratic cost function subject to linear constraints, where some of the variables are constrained to be binary.

4.3 *Simulations of MPC Semi-Active Suspensions*

The performance of the derived MPC controller was simulated for the two shock tests described in Section 3.3 with no road disturbances as well as for a "white noise" road velocity disturbance.

The shock tests simulation traces for the hybrid MPC with a control horizon N=1 were illustrated in Figures 2 and 3, where we see that indeed MPC with N=1 is identical to the "clipped optimal" control. This is expected as described below.

Consider the performance index relationship (12) between an unconstrained case and the constrained one:

$$J_{\text{semi}} = J_{\text{active,LQR}} + \int_0^{\infty} (\bar{f}_a - \bar{f})^2 dt, \tag{33}$$

We see that the model predictive control with $N = 1$ optimizes the integrand between $[t, t + dt]$. With discrete time control, this should be identical to minimize the instantaneous difference between a constrained control and the unconstrained one (LQR). Indeed, the explicit MPC control law, which will be described in the next section, is equal to the "clipped-optimal".

In Table 2, we show the performance of the MPC controller (with various design control horizons) with respect to Clipped-LQR and LQR in terms of cost function and PI values for the shock test with initial condition $x_0 = [0\ 0\ 0.1\ 0]'$. It improves beyond both "clipped-optimal" and "steepest gradient method" described in Section 3. As we can see the hybrid MPC approach can show that the "clipped-optimal" control is far from the optimal solution for this particular initial condition and constraints. It also shows that the performance of hybrid MPC is equal to the "clipped-optimal" for $N = 1$.

Table 2. Shock Test: MPC cost value for different control horizons subjected to I.C.=[0 0 0.1 0]′

N	MPC	Clipped-LQR	SGM	LQR
1	20.4282	20.4282	17.4944	0.4446
2	20.4054			
3	20.3290			
4	20.1100			
5	19.7380			
10	20.9840			
12	19.3084			
14	18.4842			
15	18.5996			
16	19.3212			
20	18.0764			
30	17.1494			
40	17.1304			

In Table 3 where the shock test starts from a different initial condition, we show that the MPC is still superior to both "clipped optimal" and "steepest gradient" as N increases. In contrast to Table 2, we see that "clipped optimal" method is superior to "steepest gradient" method in this case.

In Figure 5 we compare the power dissipated by the MPC controller with N=40 with respect to the SGM, semi-active, and active controllers for the shock test with initial condition $x_0 = [0\ 0\ 0.1\ 0]'$.

For a "white noise" road velocity disturbance, a random road disturbance described in [17] is implemented in discrete time. The road velocity w is a discrete-time noise signal normally distributed with zero mean and the standard deviation of

$$w_{RMS} = \sqrt{\frac{2 \cdot \pi \cdot v \cdot A_{road}}{T_s}}, \tag{34}$$

where $A_{road} = 4.9 \cdot 10^{-6}$, $v = 88$ [Kmh] is considered, and $T_s = 10$ [ms] is the time interval of discretization.

Considering the weights reported in Table 1, a simulation time $T = 20$ s, the above road disturbance, and a zero initial condition $x_0 = [0\ 0\ 0\ 0]'$, we compare the simulation traces of MPC with N=40 and MPC with N=1 ("clipped-optimal") in Figure 6.

In Table 4, we show the performance of the MPC controller with respect to Clipped-LQR, SGM, and LQR in terms of cost function and PI values when subject to the road velocity w as a noise signal normally distributed with mean 0 and standard deviation (34). We see that Clipped-LQR is better than SGM. And MPC with larger N is superior to both Clipped-LQR and SGM.

The MPC performance can further be visualized in the enhancement of comfort and road holding qualities as well as in the trade-off between the two. Figure 7 shows the RMS value of sprung mass acceleration (which reflects comfort) versus the RMS value of tire deflection (which reflects road holding) of various suspensions when subject to the random road disturbance described above. The optimal performance of Active-LQR with weighting factors described in Table 1 is illustrated. This performance is checked and confirmed against the design point "A" in Figure 8 of [1] since the same weighting factors and road disturbances were used. In addition, Figure 7 shows the performance of various Active-LQR controls when the weighting factor of tire deflection varies. The line populated by various Active-LQR controls with varying weighting factors describes the performance envelope of a suspension and/or the performance trade-off limitation between comfort and road holding. Figure 7 further compares the performance of the two evaluated semi-active suspensions with those of active suspensions. We see that the performance of MPC controller is closer to the performance envelope than that of clipped-optimal controller, indicating better performance in both comfort and road holding qualities.

5 Explicit Model Predictive Control

As shown in [11, 18], it is possible to compute an explicit representation $u(t) = f(x(t))$ of the receding horizon control law (31) as a collection of affine gains over (possibly overlapping) polyhedral partitions of

Table 3. Shock Test: MPC cost value for different control horizons subjected to I.C.=[0 2 0 0]′

N	MPC	Clipped-LQR	SGM	LQR
1	0.5148	0.5148	0.6198	0.2203
2	0.4744			
3	0.4629			
4	0.4558			
5	0.4547			
10	0.4482			
12	0.4446			
14	0.4427			
15	0.4427			
16	0.4427			
20	0.4419			
30	0.4404			
40	0.4398			

Table 4. Random noise:MPC cost value for different control horizons

N	MPC	Clipped-LQR	SGM	LQR
1	1.5155	1.5155	2.1361	0.1874
2	1.5474			
3	1.5445			
4	1.4579			
5	1.4416			
10	1.5238			
12	1.3079			
14	1.3160			
15	1.3083			
16	1.2886			
20	1.2204			
30	1.1456			
40	1.1462			

the set of states $x \in \mathbb{R}^4$. We denote by n_r the total number of polyhedral cells and corresponding affine gains. The explicit controller is obtained by using the Hybrid Toolbox for Matlab$^{\text{TM}}$ [10]. To compute the control law, the toolbox transforms the MLD model (30) into a piecewise affine form [19], determines all possible feasible mode sequences that are compatible with the constraints via backward reachability analysis, and employs multiparametric quadratic programming to determine candidate polyhedral regions of the solution and the corresponding value functions and optimal control gains.

If we consider a control horizon $N = 1$ we obtain $n_r = 8$ regions. A section of these regions for $x_1 = x_2 = 0$ is shown in Figure 8. The corresponding control law is

$$u(x) = \begin{cases} 10.4748x_1 + 0.2446x_2 \quad +79.1519x_3 - 3.9235x_4 \\ \quad (= K_{\text{LQ}}) \qquad\qquad\qquad \text{Regions \#1, \#6} \\ 0 \qquad\qquad\qquad\qquad\quad \text{Regions \#2, \#5} \\ (2 \cdot \zeta_{max} \cdot \omega_s)(x_4 - x_2) \quad \text{Regions \#3, \#7} \\ -1 \qquad\qquad\qquad\qquad\quad \text{Region \#4} \\ 1 \qquad\qquad\qquad\qquad\quad \text{Region \#8} \end{cases} \tag{35}$$

In regions #1 and #6 the explicit MPC control law is equal to the LQR gain. Regions #4 and #8 represent the saturated maximum dissipation constraint (8), whereas regions #3 and #7 represent the saturated maximum dissipating power constraint (9).

If we consider the control horizon $N = 2$ we obtain 62 regions, a few of which are overlapping. Techniques for reducing the number of regions without changing the control law $u(x)$ are currently under development. We do see that, despite more regions are needed as N increases, the MPC controller maintain a linear state feedback form as N increases and approaches the optimal.

6 Conclusions

For the optimal control problem of a quarter-car semi-active suspension modeled as a linear system under state dependent linear and nonlinear constraints, we have compared different semi-active control laws and proposed MPC hybrid control tools as a way for obtaining control laws with different degrees of optimality, depending on the chosen control horizon N. In particular, we have shown that for $N = 1$ the hybrid MPC law corresponds to the "clipped-optimal" control law, obtained by computing the active LQR control law and by clipping it to enforce the given constraints. Through the hybrid MPC with increased control horizon N, we also have shown that significant deviation of optimal from the "clipped optimal" can occur. We also confirmed that the optimal control law remains in an affine state feedback form. With the explicit MPC control law, we confirmed that as the control law remains affine state feedback form as it approaches optimal with increasing N.

References

[1] D. Hrovat. Survey of advanced suspension developments and related optimal control applications. *Automatica*, 33(10):1781–1817, 1997.
[2] D. Hrovat. *Optimal Passive Vehicle Suspensions*. PhD thesis, University of California, Davis, CA, 1979.
[3] D. C. Karnopp. Active damping in road vehicle suspension systems. *Vehicle System Dynamics*, 12:291–316, 1983.
[4] D. Margolis. The response of active and semi-active suyspensions to realistic feedback signals. *Vehicle System Dynamics*, 12:317–330, 1983.
[5] D. Horvat, D.L. Margolis, and M. Hubbard. An approach toward the optimal semi-active suspension. *ASME Journal of Dynamic System, Measurement, and Control*, 110(3):288–296, 1988.
[6] H.E. Tseng and J.K. Hedrick. Semi-active control laws optimal and sub-optimal. *Vehicle System Dynamics*, 23(7):545–569, 1994.
[7] P.J. Antsaklis. A brief introduction to the theory and applications of hybrid systems. *Proc. IEEE, Special Issue on Hybrid Systems: Theory and Applications*, 88(7):879–886, July 2000.
[8] A. Bemporad and M. Morari. Control of systems integrating logic, dynamics, and constraints. *Automatica*, 35(3):407–427, March 1999.
[9] F.D. Torrisi and A. Bemporad. HYSDEL — A tool for generating computational hybrid models. *IEEE Trans. Contr. Systems Technology*, 12(2):235–249, March 2004.
[10] A. Bemporad. Hybrid toolbox – User's guide. December 2003.
[11] F. Borrelli, M. Baotic, A. Bemporad, and M. Morari. An efficient algorithm for computing the state feedback optimal control law for discrete time hybrid systems. In *American Control Conference*, 2003.
[12] N. Giorgetti, A. Bemporad, H. E. Tseng, and D. Hrovat. Hybrid model predictive control application towards optimal semi-active suspension. In *Proc. IEEE Int. Symp. on Industrial Electronics*, Dubrovnik, Croatia, 2005.
[13] W.P.M.H. Heemels, B. De Schutter, and A. Bemporad. Equivalence of hybrid dynamical models. *Automatica*, 37(7):1085–1091, July 2001.
[14] G. Labinaz, M.M. Bayoumi, and K. Rudie. A survey of modeling and control of hybrid systems. In *13th IFAC World Congress 1996*, 1996.
[15] F. Borrelli, A. Bemporad, M. Fodor, and D. Hrovat. A hybrid approach to traction control. In *Hybrid Systems: Computation and Control*, Lecture Notes in Computer Science. Springer Verlag, 2001.
[16] A. Bemporad, N. Giorgetti, I. Kolmanovsky, and D. Hrovat. A hybrid system approach to modeling and optimal control of DISC engines. In *IEEE Conference on Decision and Control*, pages 1582–1587, Las Vegas, Nevada, Dec 2002.
[17] D. Hrovat and D. Margolis. Realistic road-track systems simulation using digital computers. In *Proc. of the Winter Simulation Conference*, Sacramento, December 1975.
[18] F. Borrelli, M. Baotic, A. Bemporad, and M. Morari. Dynamic programming for constrained optimal control of discrete-time linear hybrid systems. *Automatica*, 41(10), October 2005. To appear as a regular paper.
[19] A. Bemporad. Efficient conversion of mixed logical dynamical systems into an equivalent piecewise affine form. *IEEE Trans. Automatic Control*, 49(5):832–838, 2004.

Appendix A: HYSDEL List

```
/* HYSDEL List: semiactive suspension system

(C) 2003-2005 by A. Bemporad, N. Giorgetti,
    D. Hrovat, E. Tseng
*/

SYSTEM suspension {

INTERFACE {
   STATE {
      REAL x1 [-0.05,0.05];
```

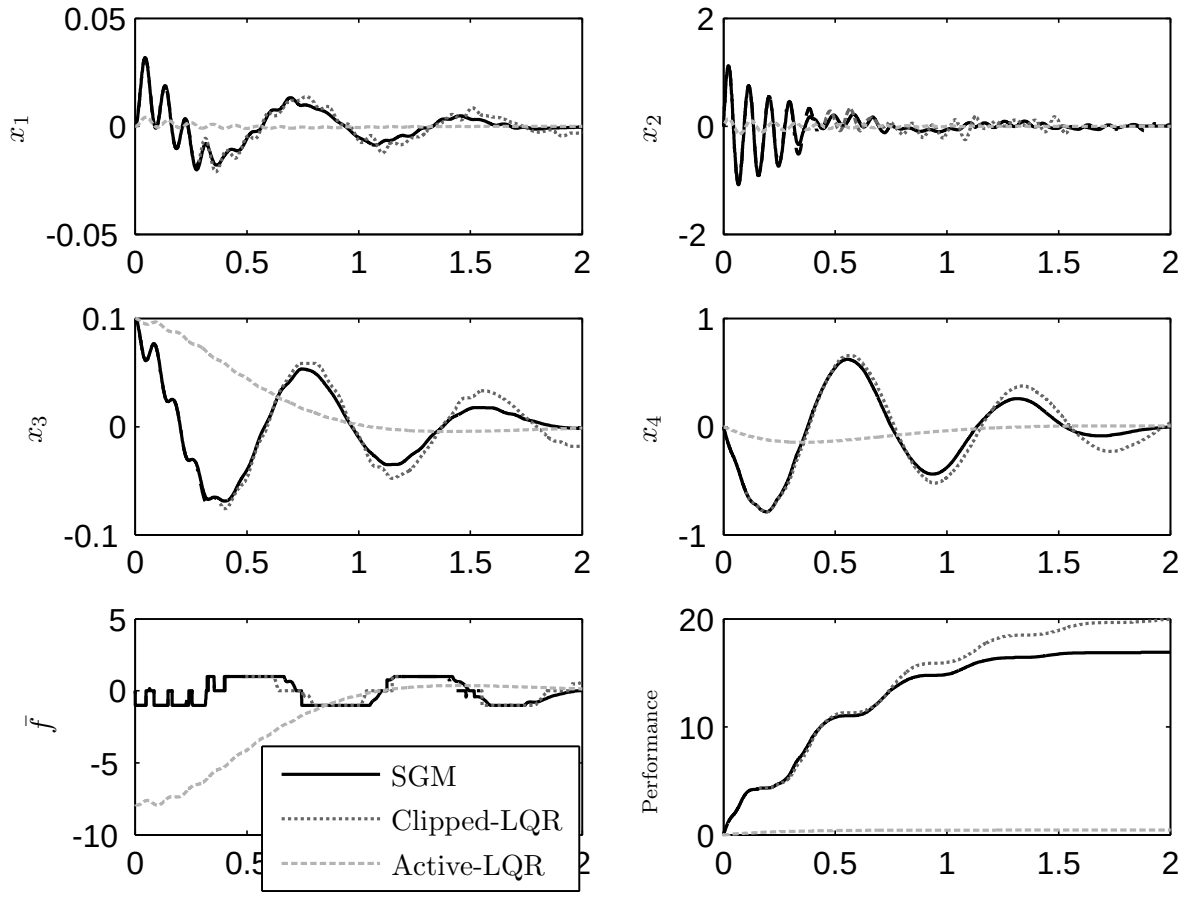

Figure 2. Shock Test of Initial Condition $x_0 = [0\ 0\ 0.1\ 0]'$ (Solid line: SGM; Dash-dotted line: clipped-LQR=MPC with horizon N=1; dashed line: Active-LQR).

```
      REAL x2 [-5,5];
      REAL x3 [-0.2,0.2];
      REAL x4 [-2,2];}
   INPUT{
      REAL u [-10,10];}
   OUTPUT {
      REAL y;}
   PARAMETER {
      REAL A1dot,A2dot,A3dot,A4dot,B4dot;
      REAL A11,A12,A13,A14,B1;
      REAL A21,A22,A23,A24,B2;
      REAL A31,A32,A33,A34,B3;
      REAL A41,A42,A43,A44,B4;
      REAL ws;}
}

IMPLEMENTATION {
   AUX {
      BOOL sign;
      BOOL usign;
      REAL F;}
   AD {
      sign = x4-x2<=0;
      usign = u<=0;}
```

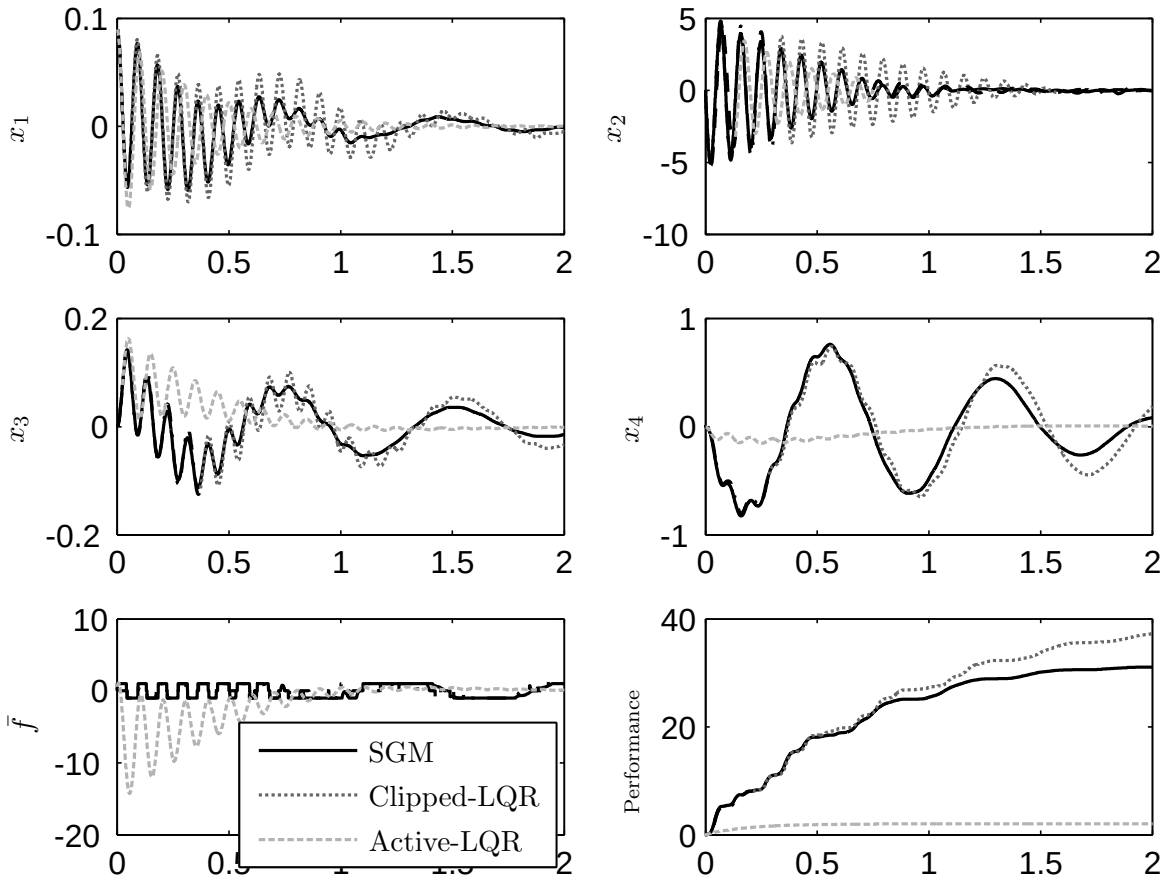

Figure 3. Shock Test of Initial Condition $x_0 = [0.09,\ 0,\ 0,\ 0]'$ (Solid line: SGM; Dash-dotted line: clipped-LQR=MPC with horizon N=1; dashed line: Active-LQR).

```
   DA {
      F={
         IF sign THEN u-(2*25.5*ws)*(x4-x2)
         ELSE -u+(2*25.5*ws)*(x4-x2)};}
   OUTPUT {
      y=A1dot*x1+A2dot*x2+A3dot*x3
        +A4dot*x4+B4dot*u;}
   CONTINUOUS {
      x1 = A11*x1+A12*x2+A13*x3
           +A14*x4+B1*u;
      x2 = A21*x1+A22*x2+A23*x3
           +A24*x4+B2*u;
      x3 = A31*x1+A32*x2+A33*x3
           +A34*x4+B3*u;
      x4 = A41*x1+A42*x2+A43*x3
           +A44*x4+B4*u;}
   MUST {
      sign -> usign;
      ~sign -> ~usign;
      F>=0;}
} }
```

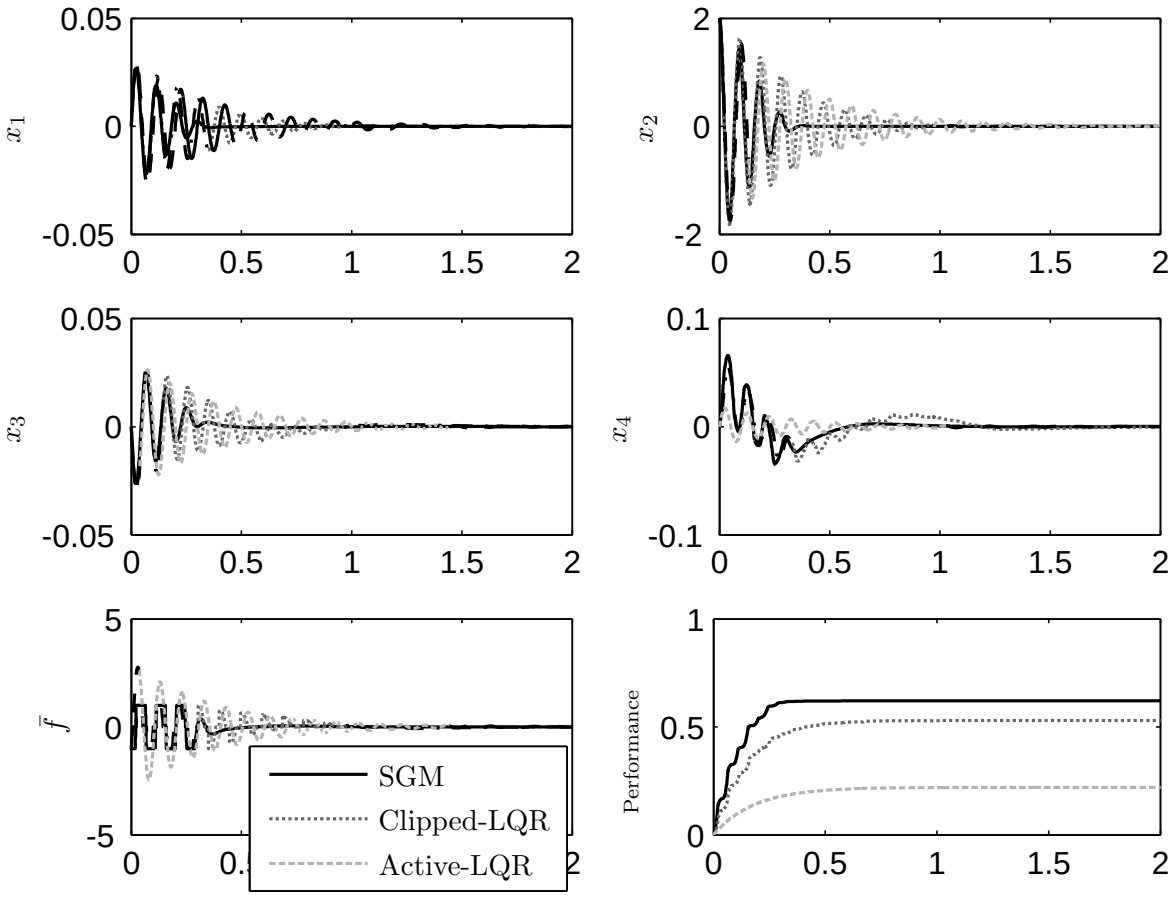

Figure 4. Shock Test of Initial Condition $x_0 = [0,\ 2,\ 0,\ 0]'$ (Solid line: SGM; Dash-dotted line: clipped-LQR=MPC with horizon N=1; dashed line: Active-LQR).

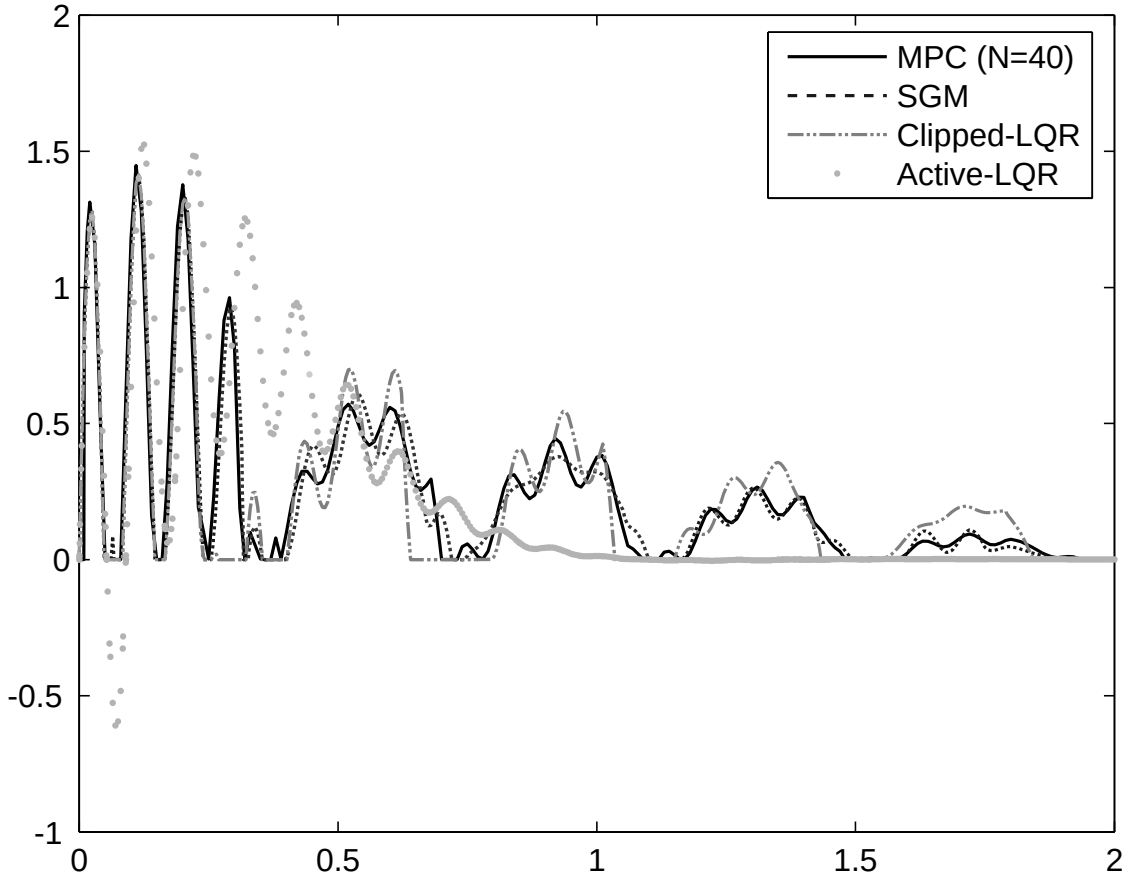

Figure 5. Power dissipated for the shock test with initial condition $x_0 = [0\ 0\ 0.1\ 0]'$ (solid line: MPC with N=40; dashed line: SGM; dash-dotted line: Clipped-LQR; dotted line: active-LQR).

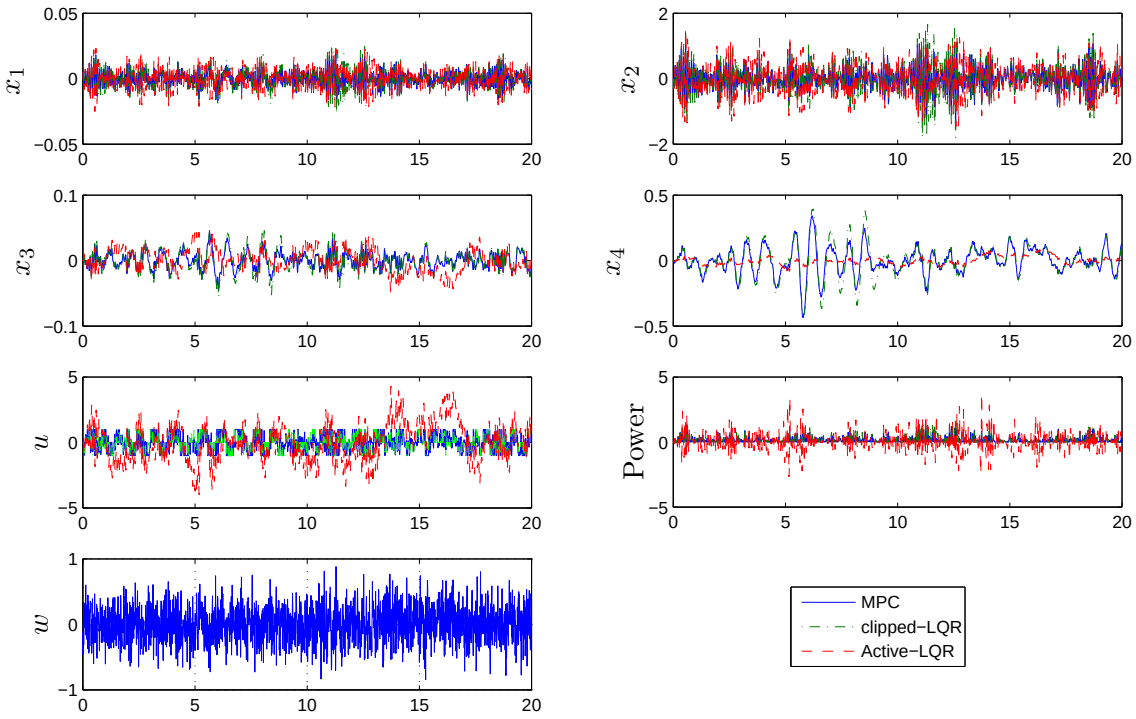

Figure 6. Closed-loop results with random noise and initial condition $x_0 = [0\ 0\ 0\ 0]'$ (solid line: MPC control with N=40; dashed line: Clipped-LQR; dash-dotted line: active-LQR)

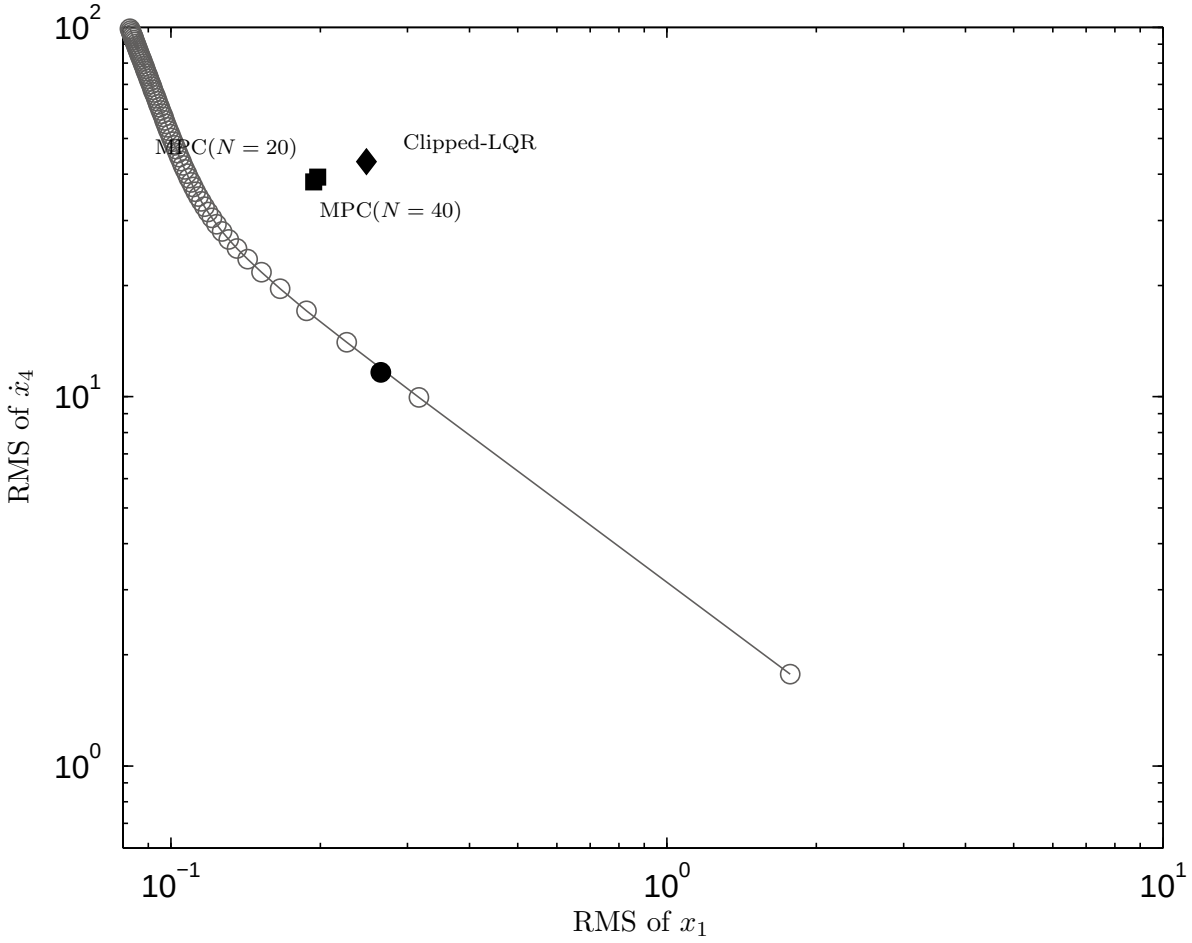

Figure 7. RMS value of sprung mass acceleration ($\dot{x}_4$) versus the RMS value of tire deflection (x_1) (solid dot: Active-LQR (w/ q_1=1100, q_3=100); hollow dot: Active-LQR control w/ varying weighting factors; diamond: Clipped-LQR; square: MPC).

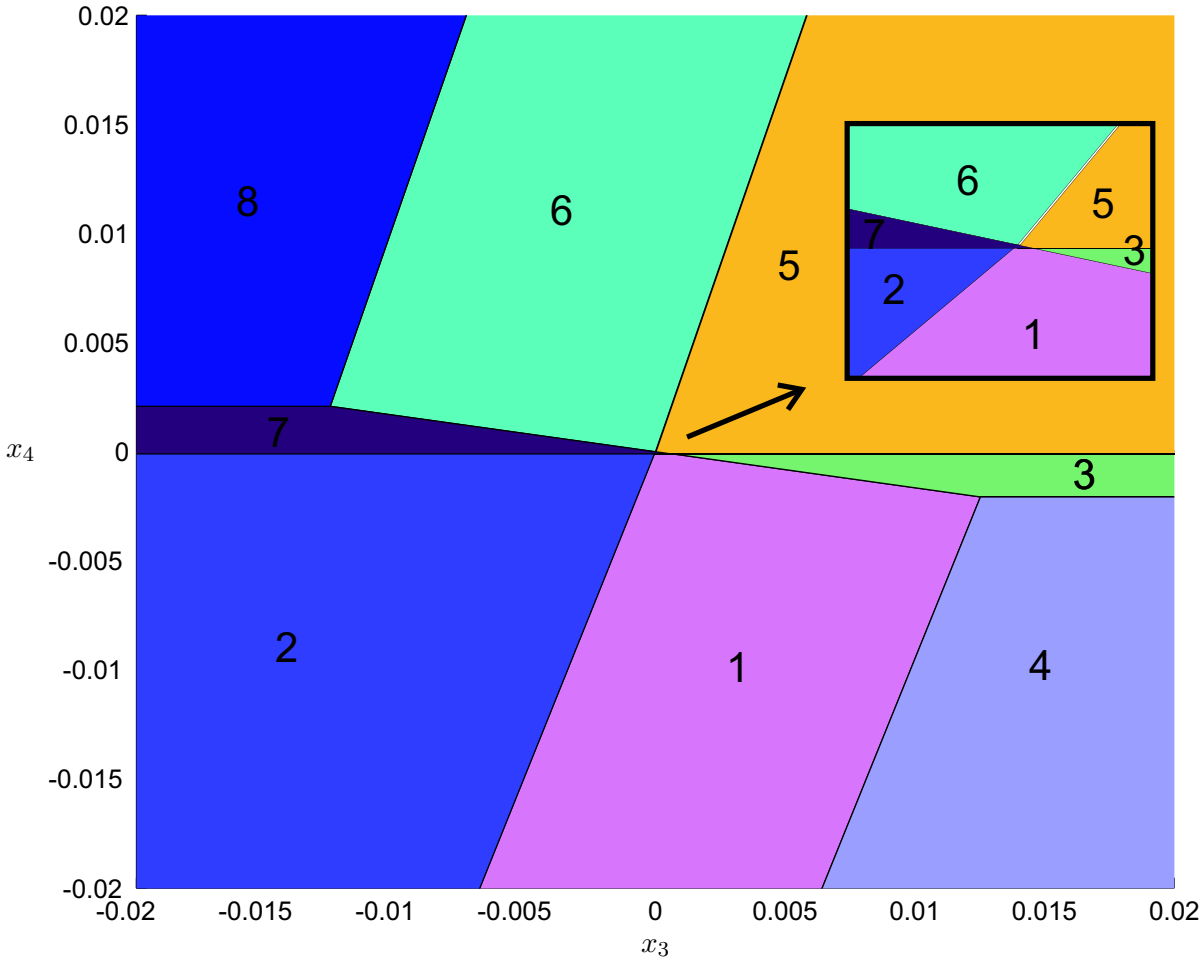

Figure 8. Plot section of the explicit controller (obtained by setting $x_1 = 0$, $x_2 = 0$).